

# Scanning Electron Microscopy

---

Volume 1985  
Number 1 1985

Article 17

---

12-1-1984

## Surface Roughness Contribution to the Auger Electron Emission

D. Wehbi

*École Nationale Supérieure de Mécanique et des Microtechniques*

C. Roques-Carmes

*École Nationale Supérieure de Mécanique et des Microtechniques*

Follow this and additional works at: <https://digitalcommons.usu.edu/electron>



Part of the [Biology Commons](#)

---

### Recommended Citation

Wehbi, D. and Roques-Carmes, C. (1984) "Surface Roughness Contribution to the Auger Electron Emission," *Scanning Electron Microscopy*. Vol. 1985 : No. 1 , Article 17.

Available at: <https://digitalcommons.usu.edu/electron/vol1985/iss1/17>

This Article is brought to you for free and open access by the Western Dairy Center at DigitalCommons@USU. It has been accepted for inclusion in Scanning Electron Microscopy by an authorized administrator of DigitalCommons@USU. For more information, please contact [digitalcommons@usu.edu](mailto:digitalcommons@usu.edu).



SURFACE ROUGHNESS CONTRIBUTION TO THE AUGER ELECTRON EMISSION

D. WEHBI and C. ROQUES-CARMES\*

Laboratoire de Microanalyse des Surfaces - ENSMM - Route de Gray  
25030 Besançon cedex - FRANCE

(Paper received June 18 1984, Completed manuscript received December 1 1984)

Abstract

Scanning Auger Microscopy (SAM) experiments have shown that  $z$  height and  $\theta$  slope relative to the analysed spot are parameters that contribute to the measured Auger intensity  $I(z, \theta)$ . For greater analysed areas specific to Auger Electron Spectroscopy (AES), the knowledge of height and slope statistical distributions  $P(z)$  and  $P(\theta)$  is required. These functions have been determined by means of profilometric data. The spatial resolution of the used tactile profilometer is similar to that which characterizes AES. A mathematical relationship  $I\{P(z), P(\theta)\}$  has been set up for Si samples whose roughness is well defined. On the other hand, Auger images can be compared to level sections.

Introduction

The importance of the surface roughness effect on Auger spectrometry has been mentioned by numerous authors {1-21, 25, 26}. In general, its contribution appears in the form of an angular factor which is difficult to establish since it occurs simultaneously during the excitation, the emission and the detection processes. However, the experimental fact which can be easily analysed on rough samples is a clear modification of the whole energetic distribution. The Auger peaks as well as the background on which they are superimposed are altered. An important series of theoretical and experimental studies {1, 9 - 15} was carried out on the correlation between the incident angle and the variations of the backscattering factor which occurs explicitly in the formulas defining the intensity of the Auger current. The correlations that were thus defined do not have any similar mathematical form on account of the different simplifying hypotheses that were used. Other angular dependent processes occur implicitly in Auger current intensity. They are those which contribute to the strict building up of the background, in particular the secondary emission {4, 17}. Bishop, in a recent publication {2}, focuses more precisely on how the background originates and how it varies with the incident angle and shows that peak/background normalization does not cancel the surface roughness effect altogether. Several other methods of background subtraction {3, 8, 16, 19, 24} or of deconvolution {21} are defined with a view to eliminating the roughness contribution as well. However, the results obtained always involve an element of uncertainty. These methods allowing a better Auger signal quantification from an energetic distribution remain approximative and in particular they do not solve the problem of the artefacts observed on Auger images {20, 25}. Moreover, owing to geometric reasons independent of the electronic processes involved, the surface roughness produces a shadowing effect which alters the detection of the emitted electrons {5, 6, 18, 19}. In the above-mentioned studies the authors consider either flat surfaces analysed through glancing incidence, or polycrystalline surfaces characterized by particular orientations. They were led to put forward simplified assumptions in order

KEY WORDS: Auger Electron Spectroscopy, Scanning Auger Microscopy, Surface roughness, Surface area, Bearing area, Height distribution, Slope distribution.

\* Address for correspondence :  
Laboratoire de Microanalyse des Surfaces  
ENSMM - Route de Gray  
25030 BESANCON CEDEX  
FRANCE Phone No. (81) 50.36.55.

to set up relationships between the complex electronic processes and the incidence angle. Let us mention two approaches which have been developed on rough surfaces correlating more directly topographic parameters to Auger intensity variations {7, 26}. Wu and Butler {26} show that Auger intensity decreases by 42 %, 58 % and 64 % as the parameter "surface area" (calculated by the Brunauer, Emmett and Teller (BET) method) increases respectively by a factor of 2.4, 2.9 and 3.6. We think that the parameter "surface area" alone cannot predict a given behavior in AES since it cannot characterize a surface topography. We can indeed observe two surfaces with different patterns and similar developed area. The results obtained by Wu and Butler seem to bear out this fact : there is a relationship between the developed area parameter and Auger intensity but it cannot be put into a mathematical form and consequently cannot be extrapolated.

Using tactile profilometry, Holloway {7} measures the height distribution function  $P(z)$  on a 2-D surface profile. He writes that Auger intensity can be directly linked to the slope distribution function  $P(\theta)$  approximately calculated from  $P(z)$ , assuming the latter gaussian distribution. We intend to bring in corrective factors directly derived from 3-D metrology, which would allow Auger intensity alterations on any sample to be quantified through the knowledge of its surface topography. Our approach consists in calculating the developed area parameter as well as the  $P(z)$  and  $P(\theta)$  functions which are not always gaussian, not from a 2-D profile but from a 3-D surface cartography with similar dimensions to those analysed in AES. To account for the detection angle, we calculate a slope distribution function  $P(\beta)$  defined with respect to the analyser axis. We think that an elementary surface observed in certain conditions in AES (incidence angle =  $\theta$ , detection angle =  $\beta$ ) is completely described by the product  $P(z) \cdot P(\theta) \cdot P(\beta)$ . SD : one point of this surface will have a certain contribution directly proportional to the probability 1) of being at  $z$  height 2) of being seen under the  $\theta$  angle by the incident beam and under the  $\beta$  angle by the detector.

The developed area parameter SD would be a factor of integration on the whole set of points building up the surface.

Furthermore, we make "level sections" in the considered area that we compare with Auger images relative to the same surface. To this end, we use a computerized tactile profilometer with a 2  $\mu$ m stylus radius whose lateral resolution is close to that which characterizes macroscopic AES (1-3  $\mu$ m) by scanning surfaces of similar dimensions to those that are scanned in AES or SAM (from 400  $\mu$ m<sup>2</sup> to a few more mm<sup>2</sup>).

Surface Roughness Criteria

3-D Representation

The 3-D surface cartography is obtained by scanning specimens using two stepping motors with a sampling length  $p$  along the  $x$  or  $y$  axis. A transducer measures the height  $z(x, y)$  referring to a standard level. The output voltage signal is digitized and stored in a computer {22}-{23}. The general scheme for the acquisition and analysis of

the data regardless of the measuring device (stylus or optical profilometer) has been presented and discussed in a previous paper {20}. Our experiments have been carried out on a Talysurf-5 stylus profilometer which was monitored by an Apple II microcomputer. The interface card is a CAN 8 or 12 bits. The data were stored on a 207 x 207 matrix. To make the 3-D cartography more attractive on a planar drawing we have projected the  $y$  values on a 45° perspective angle. The hidden surfaces were systematically deleted from the cartography in order to bring out the correct relief.

Elimination of Shape Defect

Before any statistical treatment can be applied we have to tilt the surface representation in order to make its general direction parallel to the  $(x, y)$  plane. To achieve this new surface representation we apply the following :

$$z(x,y) - Z(x,y) \tag{1}$$

where

$$Z(x,y) = D0 + D1.x + D2.y \tag{2}$$

is the least squares plane. The parameters  $D0, D1, D2$  are determined by assuming that

$$M = \sum_i \sum_j \{z(x_i, y_j) - Z(x_i, y_j)\}^2 \tag{3}$$

must be a minimum that is

$$\frac{\partial M}{\partial D0} = \frac{\partial M}{\partial D1} = \frac{\partial M}{\partial D2} = 0 \tag{4}$$

Developed Area

The surface area of a sample is given by

$$S = \sum \Delta s \tag{5}$$

where  $\Delta s$  is the area of the elementary quadrilateral whose apexes are

$A(x_i, y_i, z_{i,i}), B(x_{i+1}, y_i, z_{i+1,i}), C(x_{i+1}, y_{i+1}, z_{i+1,i+1}), D(x_i, y_{i+1}, z_{i,i+1})$  (fig. 1).  $\Delta s$  is calculated by the sum of the areas of the adjacent triangles ABC and ADC, that is

$$\Delta s = \frac{p}{2} \{ (z_{i,i+1} - z_{i,i})^2 + (z_{i+1,i} - z_{i,i})^2 + p^2 \}^{1/2} + \frac{p}{2} \{ (z_{i+1,i} - z_{i+1,i+1})^2 + (z_{i,i+1} - z_{i+1,i+1})^2 + p^2 \}^{1/2} \tag{6}$$

The "developed area" parameter SD is defined as the ratio of the surface to the geometric area :

$$SD = \frac{S}{N^2 p^2} \tag{7}$$

where  $p$  represents the sampling length and  $N^2$  is the total number of the measurement points.

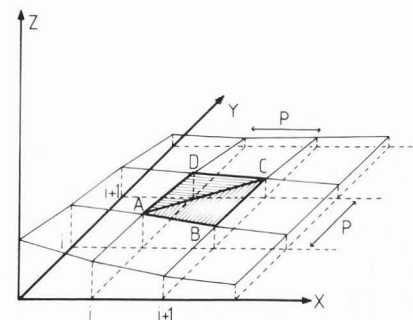


Fig. 1 : Illustration of the means of calculation of the developed area from a digitized cartography.

Level Sections

We can visualize the bearing area by cutting the surface at different z levels. The result is printed in the form of an all or none representation and quantified by the cumulative density function  $P(z)$  (bearing area). This representation is similar to that which characterizes a selective Auger image.

Experimental Results

In order to correlate surface topography to Auger emission we have carried out two sorts of experiments: one using a stylus technique for defining "surface roughness" and the other bringing out the variations of Auger intensity measured punctually on rough samples. We have already published results relative to Au and Al samples [20], [25]. Here are presented those regarding Si samples mechanically polished with emery paper 240, 600, 1000 SiC grade. Topographic Characterization

Figures 2, 3, 4 correspond to three 3-D cartographies performed in the same experimental conditions, that is, vertical magnification (X50000), scanned area ( $207 \times 207 \mu\text{m}^2$ ) and sampling length ( $1 \mu\text{m}$ ). Height histograms are superimposed on figure 5. The effect of surface finishing appears more clearly here than it does on 3-D cartography. More precisely : 1) the 240 SiC grade sample is characterized by a negatively skewed distribution indicative of more peaks than valleys. 2) a symmetrical distribution is specific to the 600 SiC grade sample, which can be interpreted as a random distribution of peaks and valleys. 3) the 1000 SiC grade sample showing a smooth surface is well defined by a sharp distribution called leptokurtic. The calculated values of the SD and Rt parameters are presented in table 1. In spite of differences in height distribution functions the SD values are close to one another. Although our results are not as sensitive as those that could be obtained by the BET technique, they provide a good characterization of the lack of developed area variations. This remark can be correlated to the small variation of the total roughness Rt experimentally determined with  $0.01 \mu\text{m}$  precision. Figures 6, 7, 8 are illustrative of the 3-D representation of the local slope modulus ( $|\vec{N}|$ ) projected on the  $\vec{Oz}$  axis. It also appears that the slope distribution functions are distinguished (figure 9). We notice that the maximum number of points is to be found at  $\theta(\vec{N}, \vec{Oz}) = 10^\circ, 15^\circ, 20^\circ$  respectively for 1000, 600, 240 SiC grade samples. What is also to be noted is that few points are located at  $\theta = 0^\circ$ . The striking fact is that the smooth sample (1000 SiC grade)--whose surface roughness is defined by :  $Rt = 1.30 \mu\text{m}$  ;  $SD = 1.01$  ; a sharp height distribution--shows an angular deviation of most local normals with regard to an expected flat surface normal. This result can account for the variations of Auger signal intensity measured on this sample. Similar singularities are observed when projecting the normal vectors on the detection direction ( $42^\circ$ ). Moreover, comparative level sections realized on the height corresponding to  $4/5 Rt$  show that the cut area increases when smoothing the surface mechanically. Figure 10 illustrates level sections made on  $50 \times 50 \mu\text{m}^2$  surfaces selected from our samples. They are comparable with Auger Images obtained by X 2000 magnification.

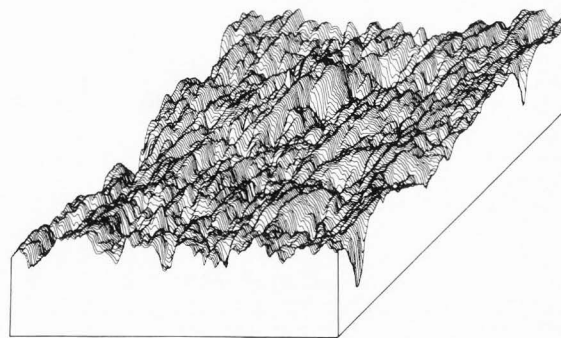


Fig. 2 : 3-D surface cartography of an Si sample mechanically polished with emery paper 240 SiC grade. Area of map is  $207 \times 207 \mu\text{m}^2$ . Sampling length is  $1 \mu\text{m}$ .

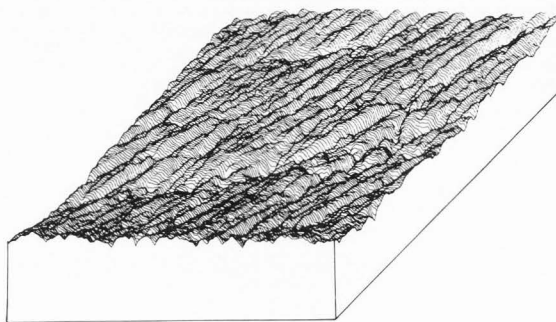


Fig. 3 : 3-D surface cartography of an Si sample mechanically polished with emery paper 600 SiC grade. Area of map is  $207 \times 207 \mu\text{m}^2$ . Sampling length is  $1 \mu\text{m}$ .

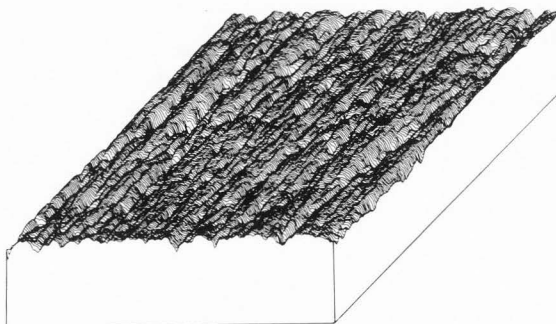


Fig. 4 : 3-D surface cartography of an Si sample mechanically polished with emery paper 1000 SiC grade. Area of map is  $207 \times 207 \mu\text{m}^2$ . Sampling length is  $1 \mu\text{m}$ .

Table 1

Variations of total roughness (Rt) and developed area (SD) parameters with the grade of the abrasive used.

	:	240	:	600	:	1000	:
	:		:		:		:
Rt ( $\mu\text{m}$ )	:	3.14	:	2.08	:	1.30	:
	:		:		:		:
SD (%)	:	102.82	:	101.83	:	101.07	:
	:		:		:		:

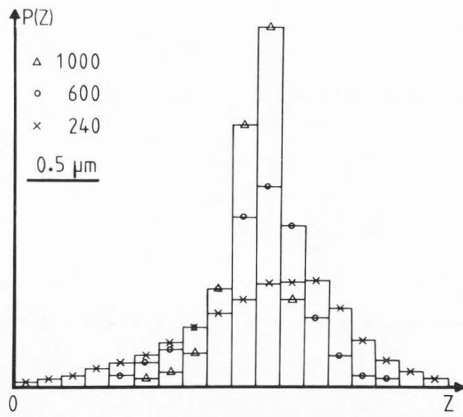


Fig. 5 : Superposition of height distribution histograms relative to the specimens shown in Figs. 2, 3, 4. On a relatively smooth surface (1000) heights are gathered around a mean value which is expressed by a sharp histogram. On the other hand a rougher surface (240) showing more height variations, is characterized by a distribution which is extended over a wider range.

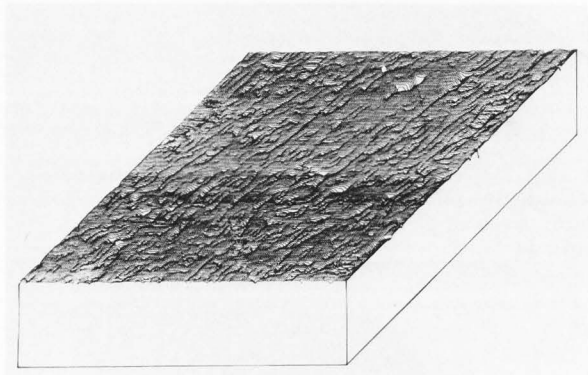


Fig. 6 : 3-D representation of the local normal vectors projected on the  $\bar{oz}$  direction. The specimen is that shown in Fig. 2.

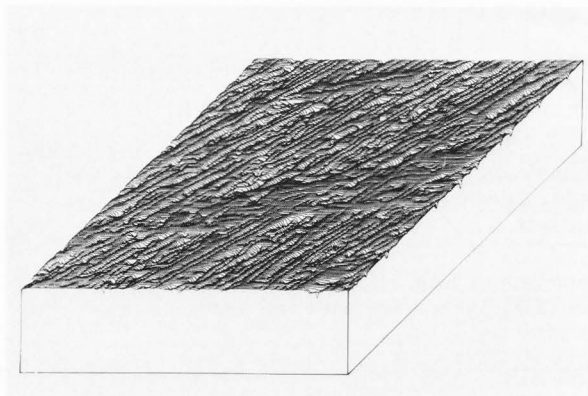


Fig. 7 : 3-D representation of the local normal vectors projected on the  $\bar{oz}$  direction. The specimen is that shown in Fig. 3.

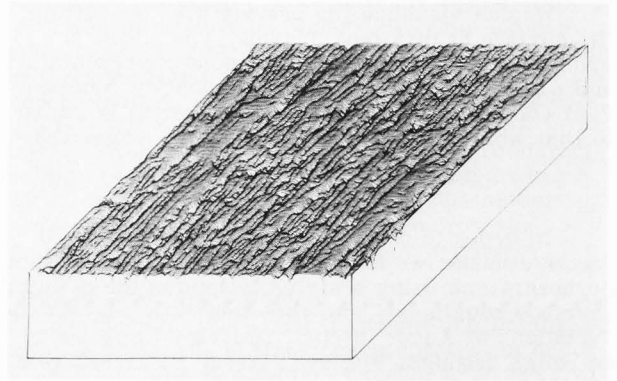


Fig. 8 : 3-D representation of the local normal vectors projected on the  $\bar{oz}$  direction. The specimen is that shown in Fig. 4.

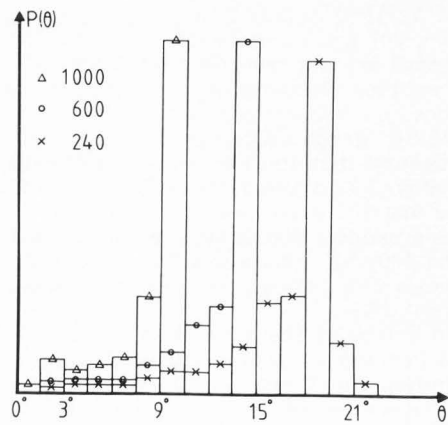


Fig. 9 : Superposition of slope distribution histograms.

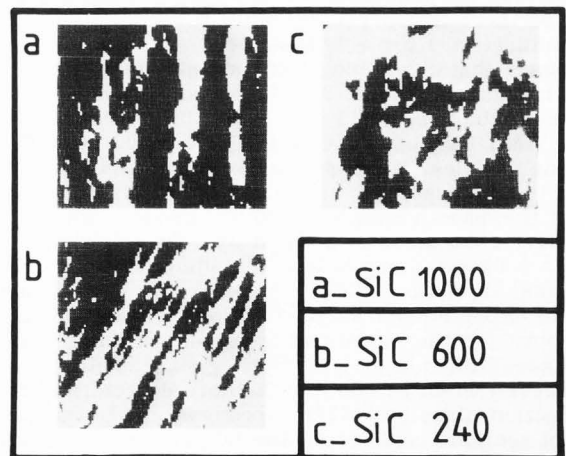


Fig. 10 : Comparative level sections realized on  $50 \times 50 \mu\text{m}^2$  surfaces on height level corresponding to  $4/5 \text{ Rt}$ .

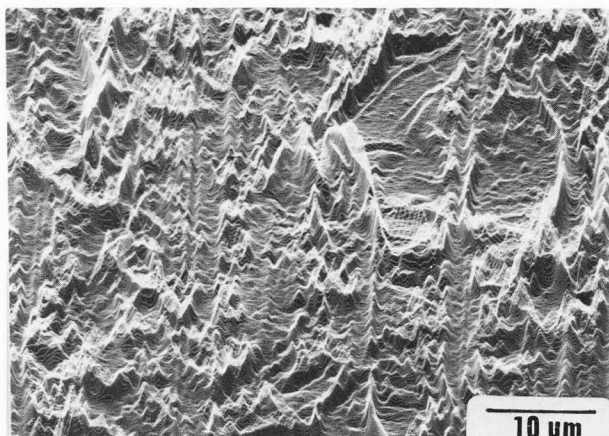


Fig. 11 : Secondary Electron Image realized on Si (600 SiC) sample, using Y deflection.  $E_p = 5 \text{ kV}$ ,  $I_p = 10^{-10} \text{ A}$ ,  $\times 2000$ .

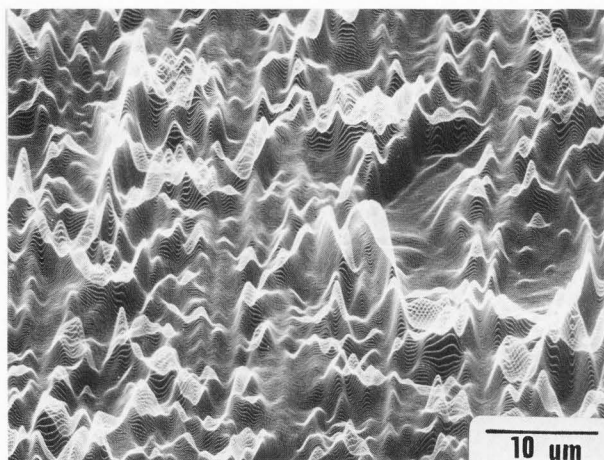


Fig. 12 : SEI realized on the same surface shown in Fig. 11, illustrating the general line profiles alteration.  $E_p = 5 \text{ kV}$ ,  $I_p = 5 \cdot 10^{-8} \text{ A}$ ,  $\times 2000$ .

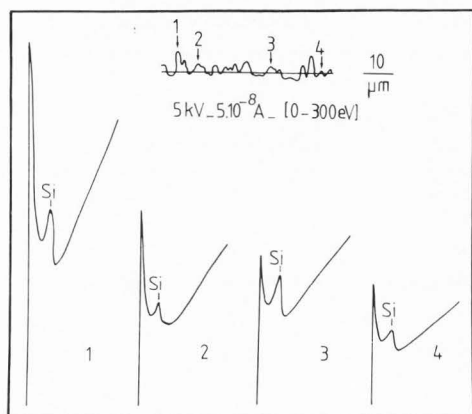


Fig. 13 : Four spectra recorded on the four indicated points along the selected SE profile.  $E_p = 5 \text{ keV}$ ,  $I_p = 5 \cdot 10^{-8} \text{ A}$ ,  $\times 2000$ . Profile 4 corresponds to that which would be expected in the case of a flat surface located at the mean height level.

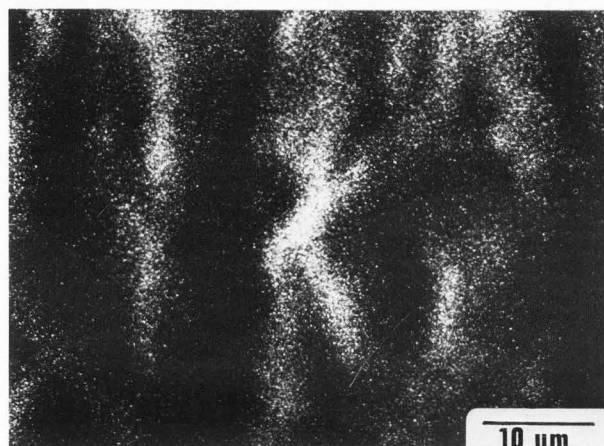


Fig. 14 : Auger Electron Image  $\text{Si}_{LVV} 89 \text{ eV}$  realized on the same surface shown in Fig. 12.

#### Punctual Auger Analysis

A more sophisticated approach of the surface roughness can be reached through Secondary Electron Images (SEI) using Y deflection (figure 11). Secondary electron images and punctual Auger analysis have been carried out on a Jamp - 10 spectrometer. However, our experimental conditions ( $E_p = 5 \text{ keV}$ ,  $I_p = 5 \cdot 10^{-8} \text{ A}$ ) alter the general line profiles (figure 12). The sharp modification of the Auger signal intensity is illustrated on recorded spectra by selecting different points on one of the SE profiles contributing to the SE image (figure 13). The whole electron distribution is enhanced on peaks and lowered on valleys. No shadowing effect or incident beam obstruction occur in these experiments for two main reasons : 1) the selected points do not have neighboring asperities. 2) The secondary signal intensity detected either by the CMA ( $42^\circ$ ) or by the Everhart detector (normal detection) is of the same order of magnitude. The silicon

Auger image ( $\text{Si}_{LVV} 89 \text{ eV}$ ) only reproduces the relief summits (figure 14).

#### Discussion and Conclusions

Using a stylus technique, we have determined the 3-D criterion or parameter evolution occurring indirectly in Auger spectroscopy. We have particularly focused our attention on a global parameter (developed area) and on statistical functions (height and slope distributions). The main experimental results could be summarized as follows : 1) The developed area, as a first order - approximation, is a parameter which can explain the deviation in relation to a flat surface in AES. However, in the case of the considered samples in which the SD values are close to one another, other criteria are to be taken into account. A function depending on height and slope distributions can explain the main results obtained. 2) The height histogram expands

with respect to the paper grade. Its width illustrates the total roughness value  $R_t$ . 3) The slope histogram calculated in relation to the  $\vec{Oz}$  or  $42^\circ$  directions is characterized by a quite different population for selective angular values which increase according to the abrasive used. 4) The level sections also show the evolution of the bearing area in relation to the surface state finishing. The greater the bearing area is, the greater the reproduced surface on the Auger image can be expected. It turns out that there is a rather important deviation on our samples compared to a strictly flat standard surface. Two different approaches are required to achieve the extrapolation of these results on Auger intensity: 1) The first approach consists in using AES both on flat standard samples and on the rough samples to be tested. In that case, the Auger intensity ratio can be written as follows:

$$\frac{I}{I_{\text{standard}}} = SD \int p(z) \cdot p(\theta) \cdot \Delta z \cdot \Delta \theta \quad (8)$$

which implies that the difference in intensities depends exclusively on topographic criteria. 2) The second approach consists in using SAM and quantifying the SE profiles which reproduce the given 2-D roughness profiles  $z(x)$ . In that particular case, the punctual determination of the Auger intensity variations can be expressed as follows:

$$\frac{I(x)}{I_{\text{standard}}} = z(x) \cdot \frac{\partial z(x)}{\partial x} \quad (9)$$

The computed secondary electron profile, recorded on pure samples, should allow  $I(x)$  to be known on condition that it is normalized by a reference signal. On non pure samples, the real roughness profile must be necessarily obtained by means of a stylus technique. As a conclusion, we can state that in every case: 1) any spectrometric analysis should be preceded by topographic investigations. 2) preliminary results show that this type of correlation agrees quite well with experimental results (Wehbi D., Thesis in progress). 3) the validity of experimental spectrometric results carried out on rough samples as well as that of the geometrical arrangement of the spectrometer used keeps raising a few problems. Better results on rough samples can be obtained by means of a coaxial CMA since, for instance, the two sides of the same asperity will be symmetrical in relation to both excitation and detection. A study on the real shadowing effect will be performed through similar experiments to those carried out at the National Bureau of standards [22].

#### Acknowledgements

The authors would like to thank Prof. Ch. Tissot for his kind contribution to the English translation.

#### References

- Baines M., Howie A., Andersen S.K. (1975); Crystalline effects in Backscattering and Auger production, *Surf. Sci.* **53**, 546-553.
- Bishop H.E. (1984); The role of the background in Auger electron spectroscopy, in: *Electron Beam Interactions with Solids*, D.F. Kyser, H. Niedrig, D.E. Newbury, R. Shimizu (eds.), SEM, Inc., P.O. Box 66507, AMF O'Hare, IL, 60666, 259-269.
- Brurrel M.C., Kaller R.S., Armstrong N.R. (1982); Data acquisition and processing modes for quantitative Auger electron spectroscopy. *Anal. Chem.* **54**, 2511-2517.
- Cook L.P., Farabaugh E.N., Olson C.D. (1979); Y-deflection modulated secondary electron images in the evaluation of ceramic surface finish. *The Science of Ceramic Machining and Surface Finishing II*, Hockey B.J. and Rice R.W. (Ed), National Bureau of Standards Special Publication, Washington D.C., **562**, 407-415.
- Gerlach R.L., Cargill R.C. (1983); An investigation of Auger electron signal as a function of sample and detector angles. *Surf. Sci.* **126**, 565-568.
- Harris L.A. (1969); Angular dependences in electron-excited Auger emission. *Surf. Sci.* **15**, 77-93.
- Holloway P.H. (1975); The effect of surface roughness on Auger electron spectroscopy. *J. Electron Spectrosc. Related Phenomena* **7**, 215-232.
- Houston J.E. (1974); Background subtraction. *Rev. Sci. Instrum.* **45** N° 7, 897-903.
- Ichimura S., Shimizu R. (1981); Backscattering correction for quantitative Auger Analysis I. *Surf. Sci.* **112**, 386-408.
- Ichimura S., Shimizu R., Ikuta T. (1982); Backscattering Correction II. *Surf. Sci.* **115**, 259-269.
- Ichimura S., Shimizu R., Langeron J.P. (1983); Backscattering Correction III. *Surf. Sci.* **124**, L 49 - L 54.
- Jablonski A. (1979); Backscattering effects in Auger electron spectroscopy: A review. *Surf. Interface Analysis* **1** N°4, 122-131.
- Jablonski A. (1983); Dependence of the Backscattering factor in AES on the primary electron incidence angle. *Surf. Sci.* **124**, 39-50.
- Janssen A.P., Harland C.J., Venables J.A. (1977); A ratio technique for micro-Auger analysis. *Surf. Sci.* **62**, 277-292.
- Kirschner J. (1976); The role of backscattered electrons in scanning Auger microscopy. *Scanning Electron Microsc.* 1976; I: 215-220.
- Langeron J.P., Minel L., Vignes J.L., Bouquet S., Pellerin F., Lorange G., Ailloud P., Le Héricy J. (1984); An important step in quantitative Auger analysis: The use of peak background ratio. *Surface Science* (in press).
- Mc Adams H.T. (1974); Scanning electron microscope and the computer: New tools for surface metrology. *Modern Machine Shop*. June, 82-91.
- Pendry J.B. (1975); Angular dependence of electron emission from surfaces. *J. Phys. C Solid State Phys.* **8**, 2413-2422.
- Prutton M., Larson L.A., Poppa H. (1983); Techniques for the correction of topographical effects in scanning Auger electron microscopy. *J. Appl. Phys.* **54**(1), 374-381.
- Roques-Carmes C., Wehbi D., Mairey D., Cabala R. (1983); les effets de la topographie

de surface en spectrométrie Auger. Influence of surface topography on Auger electron spectroscopy. *Le Vide, les Couches Minces*, 216, 221-231.

21. Sickafus E.N. (1980) ; A secondary electron emission correction for quantitative Auger yield measurements. *Surf. Sci.* 100, 529-540.
22. Teague E.C., Scire F.E., Baker S.M., Jensen S.W. (1982) ; Three-dimensional stylus profilometry. *Wear* 83, 1-12.
23. Thomas T.R. (1982) : *Rough Surfaces*. Thomas T.R. (Ed) Longman Inc., New York, 144-166.
24. Todd G., Poppa H. (1978) ; Some performance tests of a microarea AES. *J. Vac. Sci. Technol.* 15(2), 672-674.
25. Wehbi D., Roques-Carnes C. (1984) ; The effects of surface roughness on Auger electron spectroscopy. *Journal de Physique*, 45 C2, 319-322.
26. Wu O.K.T., Butler E.M. (1982) ; Auger signal intensity dependence on surface area (roughness). *J. Vac. Sci. Technol.* 20(3), 453-457.

Discussion with Reviewers

J. Kirschner : Are you able to perform a statistical analysis similar to that of the surface topography on the Auger maps and what result would you expect ?

Authors : Over the past three months we have achieved a software allowing us to perform a similar statistical analysis on Secondary, Back-scattered and Auger Electron Images or profiles. The recorded Secondary Electron profiles are not always as smooth as those presented here. However a smooth profile identical to those obtained by means of a stylus technique is characteristic of backscattered and Auger electron profiles. In a previous paper (20) we have illustrated this evolution with respect to experimental conditions. However, we have to bear in mind that the use of a stylus technique remains compulsory for the roughness measurement of chemically heterogeneous surfaces.

M.P. Seah : A major defect to the tactile technique is the poor response of the stylus with a 2  $\mu\text{m}$  radius to roughness which, seen in the scanning electron microscope is not nearly as smooth as seen here in the profile maps. The bias in  $P(z)$  and the reduction in  $P(\theta)$  clearly result from the effect of the stylus tip. To obtain a true reproduction of  $P(z)$  and  $P(\theta)$  the authors must either deconvolute the stylus function from the results (not a strict deconvolution) or build a Raster Scanning Tunnelling Microscope. Do the authors have any comments ?

Authors : Let us mention again that, in a first stage, the selection of a tactile profilometer is based on the following facts 1) the lateral resolution of the used stylus, which is by no means comparable to that of a scanning electron microscope, is still similar to that which characterizes AES. 2) topographic results can be obtained even on chemically heterogeneous samples. Ever since our investigation began, special attention has been focused on the stylus transfer

function. Sinusoidal functions have been used for simulating rough profiles. This is, in our opinion, a realistic approach since every real profile can be described in terms of a Fourier series. We have shown in particular 1) that the frequencies of the sampled function are not, in any case, fully reproduced 2) peaks are more enhanced than valleys 3) a real profile can be fully reproduced on condition that its amplitude must be greater than 15  $\mu\text{m}$  and its wavelength greater than 9  $\mu\text{m}$ . In the next stage we plan to investigate the same samples by means of various optical profilometers which have already been set up in our Laboratory and which have so far provided a better resolution.

L. Church : Which of the two approaches outlined provides a better way to correct for sample roughness ?

Authors : Surface topography is directly involved in the detection function and indirectly involved in the emission function. In fact, the measured intensity can be considered as the product of three functions : excitation, emission and detection. A corrective factor either dependent on  $z$ ,  $\theta$  or on  $P(z)$ ,  $P(\theta)$  allows in a first approximative approach the whole cancellation of detection artefacts and the partial cancellation of excitation and emission artefacts. It turns out that a true corrective factor will be introduced when we consider the fractal dimension of the analysed surfaces. The latter approach is being developed in our Laboratory.

L. Church : What are the physical dimensions associated with the ordinate of the SE insert in Fig. 13 ?

Authors : Arbitrary units have so far been plotted on the ordinate axis. In order to obtain quantitative data an electronic scale adaptor has been devised. It allows the input/output signal to be defined in digit/ $\mu\text{m}$  units.

J. Kirschner : The intensity of the low energy Auger peak seems to scale with the total secondary electron production. Does this hold also for the high energy peaks and/or the intensity from an overlayer such as a thin oxide film ?

Authors : This enhancement effect has been observed over the whole energetic distribution and consequently for the high energy peaks. Similar analytical facts have been noticed on rough samples covered with oxide films or coatings.

L.L. Levenson : According to your results, both theoretical and experimental, one should expect a relatively intense Auger signal for a high sharp feature. You state that no shadowing was observed in your Figure 13, even with the JAMP-10. In your Figure 14, only the crests of high features are imaged with the  $\text{Si}_{1VV}89$  eV peak. Can you, therefore, clarify what "better results" may be expected from a coaxial CMA ? Have such "better results" been observed ?

Authors : As regards all surfaces involving geometrical symmetry such as sinusoidal shapes, a coaxial CMA should provide a better electron detection and cancel the shadowing effect as well. In our experimental set up, we bring in corrections through a software in order to obtain more realistic results.



